Rare Metal Materials and Engineering
Volume 49, Issue 5, May 2020
Available online at www.rmme.ac.cn

Science Press

Cite this article as: Rare Metal Materials and Engineering, 2020, 49(5): 1539-1545.

ARTICLE

Experimental Investigation of the Phase Equilibria in the Ni-Co-Sn Ternary System

Liu Xingjun[1, 2], **Deng Yuling**[1], **Zhang Jinbin**[1], **Yang Mujin**[1], **Yang Shuiyuan**[1], **Han Jiajia**[1], **Lu Yong**[1], **Wang Cuiping**[1]

[1] *College of Materials, Fujian Provincial Key Laboratory of Materials Genome, Xiamen University, Xiamen 361005, China;* [2] *Harbin Institute of Technology, Shenzhen 518055, China*

Abstract: Phase equilibria of the Ni-Co-Sn ternary system at 700 °C and 1000 °C were experimentally determined by using electron probe microanalyzer and X-ray diffraction. No ternary compound was found at 700 °C and 1000 °C. There was an extensive region of mutual solubility existing between βCo_3Sn_2 phase and Ni_3Sn_2(*h*) phase. Three Ni-Sn binary compounds [Ni_3Sn(*l*), Ni_3Sn(*h*) and Ni_3Sn_4] showed absolutely different solubilities for the element Co. The maximum solubility of Co in Ni_3Sn(*l*) and Ni_3Sn_4 phases at 700 °C were 6.9 at% and 25.6 at%, respectively, and the solubility of Ni_3Sn(*h*) phases changed into 15.5 at% at 1000 °C. The Ni-Co side presented an interconnected (αCo, Ni) phase region at both 700 and 1000 °C and its homogeneity range for Sn was from 1 at% to 10.5 at%. The solubility of Ni in the linear compound CoSn phase was about 15.9 at%.

Key words: Ni-Co-Sn ternary system; phase diagram; linear compound

Lead-free soldering plays an important role in the electronic packaging industry[1-4]. During the soldering process, interfacial reactions will occur at the soldering joint among Ni, Co and Sn elements[5]. Additionally, the additions of Ni and Co elements can improve the overall performance of lead-free solders[6-8]. According to the results of Huang, Chen et al.[9,10], the addition of a small amount of Co can significantly reduce the overcooling effect and effectively refine the microstructure of the solder. In order to study the lead-free solder and the interfacial reactions on Ni and Co substrate, it is important to determine the Ni-Co-Sn ternary equilibria experimentally.

The corresponding sub-binary systems of Ni-Co-Sn ternary system, have been well studied. The Co-Ni phase diagram is a very simple system without any intermetallic compounds which has been reported by S. U. Jen and R. Kainuma. An infinite mutual solubility of Co and Ni has been found[11,12]. Co-Sn phase diagram has been reported by M. Jiang which demonstrated four stable compounds $CoSn_2$, CoSn, αCo_3Sn_2, βCo_3Sn_2[13]. The Ni-Sn binary system has been widely studied as an important lead-free soldering material system[14], and assessed by Ghosh[15], Liu[16] and Dong[17] et al. Ni-Sn phase diagram has been reported by A. Zemanova[18] which demonstrated five stable compounds Ni_3Sn(*l*), Ni_3Sn(*h*), Ni_3Sn_2(*l*), Ni_3Sn_2(*h*), Ni_3Sn_4. The 250 °C isothermal section of the Ni-Co-Sn ternary system is proposed by Y. H. Chao[3]. In their research, it is worthy to pay attention to the fact that both intermetallic compounds: the βCo_3Sn_2 phase (in the Co-Sn system), and the Ni_3Sn_2(*h*) phase (in the Ni-Sn system), have the same orthorhombic structure. There is an extensive region of mutual solubility existing between the two binary isomorphous phases, βCo_3Sn_2 and Ni_3Sn_2(*h*).

The three binary phase diagrams of Co-Ni, Co-Sn and Ni-Sn constituting the Ni-Co-Sn ternary system are shown in Fig.1 and the information of stable solid phases and their crystal structures in three binary systems are summarized in Table 1.

Although there are a large number of investigations about the above subsystems, the experimental equilibria of the Ni-Co-Sn ternary system is still scarce. Up to now, there is only one phase diagram of the Ni-Co-Sn ternary system at 250 °C[3]. Despite the fact that soldering temperature is usually lower than 450 °C, it is necessary to obtain the phase equilib-

Received date: June 25, 2019
Foundation item: National Natural Science Foundation of China (51771158); Joint Fund to Promote Cross-Strait Scientific and Technological (U1605243)
Corresponding author: Wang Cuiping, Ph. D., Professor, Department of Materials Science and Engineering, College of Materials, Xiamen University, Xiamen 361005, P. R. China, Tel: 0086-592-2180606, E-mail: wangcp@xmu.edu.cn

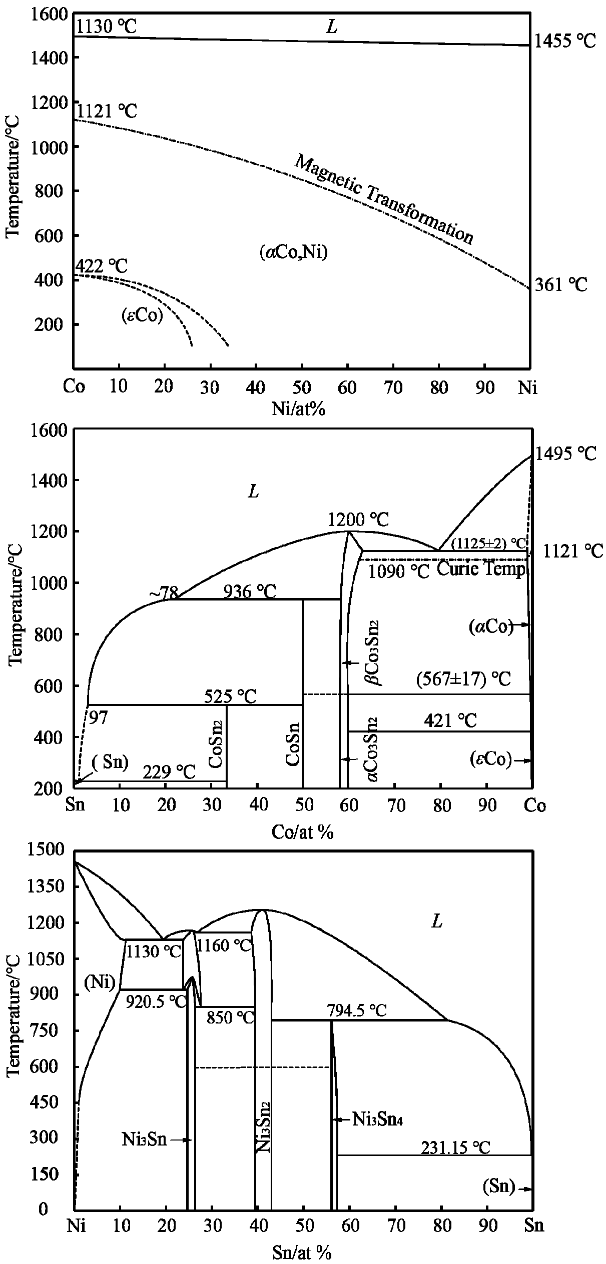

Fig.1 Binary phase diagrams constituting the Ni-Co-Sn ternary system[11,13,18]

rium information at high temperature, and it will provide a theoretical basis for the thermodynamic calculation of the Ni-Co-Sn ternary system.

1 Experiment

Pure metals Nickel (99.9 wt%), Cobalt (99.9 wt%) and Tin (99.9 wt%) were used as raw materials and the bulk buttons were prepared by arc melting under high purity argon atmosphere. The mass of each sample was about 15 g. In order to achieve their homogeneity, the ingots were remelted at least 4 times and the mass losses were less than 0.5 wt%.

Table 1 Stable solid phases in the three binary systems[11, 13, 18]

Phase	Pearson symbol	Prototype	Space group	Struktur-bericht
(αCo,Ni)	*cF4*	Cu	*Fm-3m*	*A*1
(εCo)	*hP2*	Mg	$P6_3/mmc$	*A*3
(αCo)	*cF4*	Cu	*Fm-3m*	*A*1
(εCo)	*hP2*	Mg	$P6_3/mmc$	*A*3
(βSn)	*tI4*	βSn	$P4_1/amd$	*A*5
(αSn)	*cF8*	C(diamond)	*Fd-3m*	...
βCo_3Sn_2	*hP6*	Ni_2In	$P6_3/mmc$	$B8_1$
αCo_3Sn_2	*oP20*	Ni_3Sn_2	*Pnma*	$B8_1$
CoSn	*hP6*	CoSn	*P6/mmm*	*B35*
$CoSn_2$	*tI12*	$CuAl_2$	*I4/mcm*	*C16*
$\beta CoSn_3$	*tI64*	$\beta CoSn_3$	$I4_1/acd$	*A2*
$\alpha CoSn_3$	*oC32*	$PdSn_3$	*Cmca*	...
Co_3Sn	*cI2*	W	*Im-3m*	*A2*
(Ni)	*cF4*	Cu	*Fm-3m*	*A*1
(βSn)	*tI4*	βSn	$P4_1/amd$	*A*5
(αSn)	*cF8*	C(diamond)	*Fd-3m*	...
$Ni_3Sn(h)$	*cF16*	$BiF_3{}^b$	*Fm-3m*	$D0_3$
$Ni_3Sn(l)$	*hP8*	Mg_3Cd	$P6_3/mmc$	$D0_{19}$
$Ni_3Sn_2(h)$	*hP6*	$InNi_2$	$P6_3/mmc$	$B8_1$
$Ni_3Sn_2(l)$	*oP20*	Ni_3Sn_2	*Pnma*	$B8_1$
Ni_3Sn_4	*mC14*	CoGe	*C2/m*	...

The ternary Ni-Co-Sn alloys were cut into small pieces and then put into quartz capsules and filled with argon gas. In addition, the samples containing liquid phase were wrapped in pure Nickel slice to prevent the contact reaction with quartz. Specimens were annealed at 700 °C for 720 h and 1000 °C for 168 h. And the samples which are containing liquid phase were annealed 700 °C for 5 h and 1000 °C for 2 h. Specimens were quenched into ice water after heat treatment.

After standard metallographic preparation, the backscatter electron (BSE) images and equilibrium composition of the equilibrium phases were obtained on electron-probe- micro-analyzer (EPMA, JXA-8100, JEOL, Japan). High purity metals were used as standard metallographic and the measurements were carried out at a voltage of 20 kV and a current of 1.0×10^{-8} A. The crystal structure analysis was conducted using X-ray diffraction (XRD) on a Philips Panalytical X-pert diffractometer (Cu Kα radiation at 40 kV and 40 mA). The data were collected in the range of 2θ from 20° to 90° at a step size of 0.0167°.

2 Results and Discussion

2.1 An extensive region of mutual solubility

According to Y. H. Chao's study[3], it is worthy to pay attention to the fact that both intermetallic compounds: the βCo_3Sn_2 phase (in the Co-Sn system), and the $Ni_3Sn_2(h)$ phase (in the Ni-Sn system), not only have the same orthorhombic structure, but also have very similar values in terms of lattice parameters.

Therefore, it is reasonable to speculate that there is an extensive region of mutual solubility between βCo_3Sn_2 and $Ni_3Sn_2(h)$. For the validation of the existence of a continuous solid solution between βCo_3Sn_2 and $Ni_3Sn_2(h)$ phases in the isothermal section of the Ni-Co-Sn ternary system at 700 °C, three different alloys ($Ni_{16}Co_{42}Sn_{42}$, $Ni_{29}Co_{32}Sn_{39}$, $Ni_{44}Co_{18}Sn_{38}$) in this single-phase region were prepared. Their BSE micrographs show the appearance of a single phase and their compositions determined using EPMA. Their XRD results are shown in Fig.2, where the characteristic peaks of the βCo_3Sn_2 and $Ni_3Sn_2(h)$ phases are only confirmed and well marked by star symbols. Based on the analyses of EPMA and XRD, an extensive region of mutual solubility existing between βCo_3Sn_2 and $Ni_3Sn_2(h)$ was confirmed and labeled as (Ni, Co)$_3$Sn$_2$.

2.2 Phase equilibria at 700 °C

Typical BSE images of the Ni-Co-Sn equilibrated alloys quenched from 700 ^{o}C are shown in Fig.3a~3f while their phase equilibrium compositions are listed in Table 2. All the mentioned chemical compositions in this work is given in the form of an atomic ratio (at%). Phase identification was based on the equilibrium composition as measured by EPMA and XRD results. Most of the identification of equilibrium phases could be confirmed by taking advantage of the available composition ranges and crystal structure information of the intermetallic compounds in the binary and ternary systems[11,13,18].

The $Ni_{11}Co_{70}Sn_{19}$ alloy annealed at 700 °C for 720 h has formed a eutectic organization of (Ni, Co)$_3$Sn$_2$ and (αCo, Sn) phases, as illustrated in Fig.3a. This sample composition crosses the eutectic reaction line during the cooling process; therefore, a eutectic reaction occurred and a strip phase (αCo, Sn) was formed. The corresponding XRD pattern, as presented in Fig.4a, shows all the diffraction peaks of the (αCo, Sn) and (Ni, Co)$_3$Sn$_2$ phases. Fig.3b shows the two-phase microstructure (Ni_3Sn_4+Liquid phase) of the $Ni_{20}Co_{20}Sn_{60}$ alloy annealed at 700 °C for 5 h. The BSE image of $Ni_{62}Co_{11}Sn_{27}$ alloy

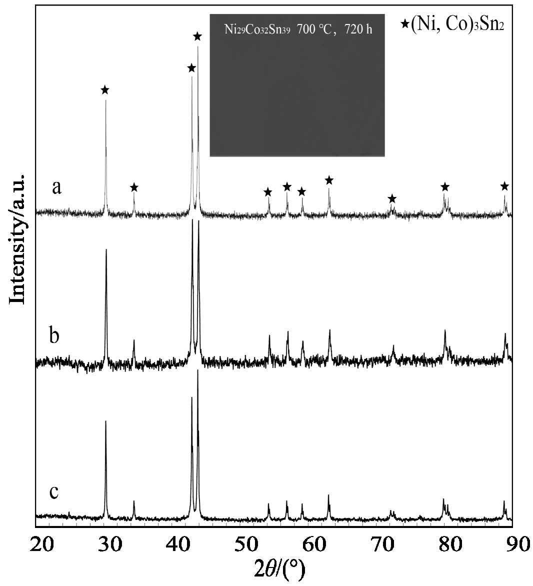

Fig.2 XRD patterns of partial Ni-Co-Sn ternary alloys annealed at 700 °C for 720 h obtained from $Ni_{16}Co_{42}Sn_{42}$ (a), $Ni_{29}Co_{32}Sn_{39}$ (b), and $Ni_{44}Co_{18}Sn_{38}$ (c)

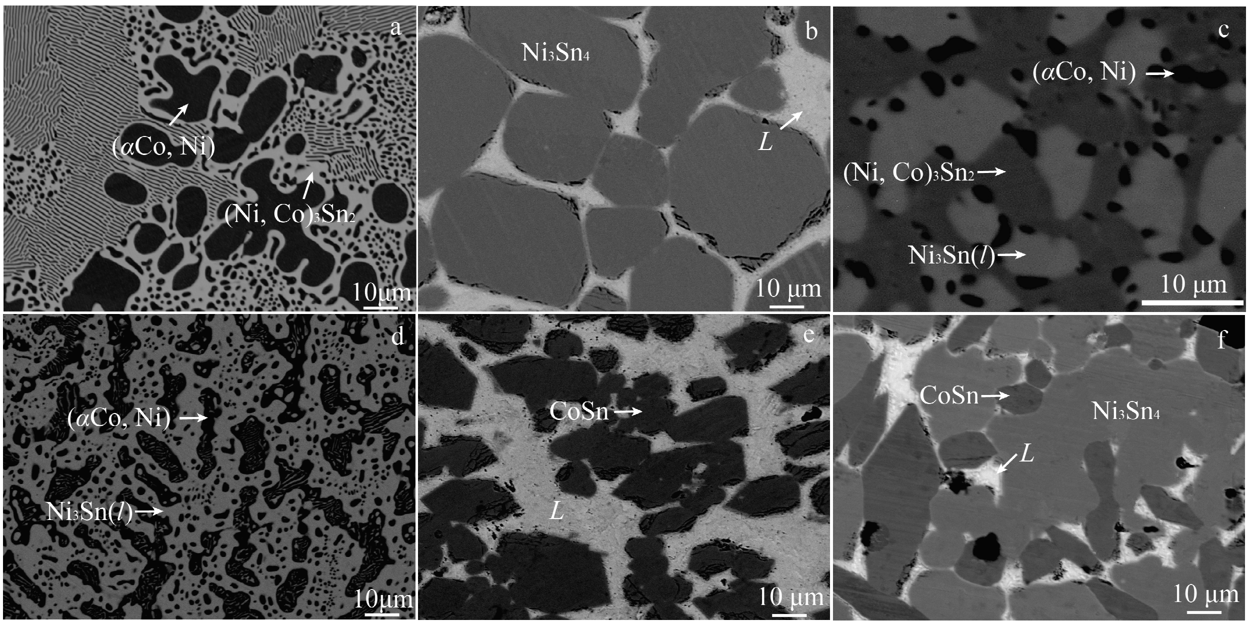

Fig.3 Typical ternary BSE images obtained from Ni-Co-Sn ternary alloys: (a) $Ni_{11}Co_{70}Sn_{19}$ alloy annealed at 700 °C for 720 h, (b) $Ni_{20}Co_{20}Sn_{60}$ alloy annealed at 700 °C for 5 h, (c) $Ni_{62}Co_{11}Sn_{27}$ alloy annealed at 700 °C for 720 h, (d) $Ni_{75}Co_{11}Sn_{14}$ alloy annealed at 700 °C for 720 h, (e) $Ni_{10}Co_{30}Sn_{60}$ alloy annealed at 700 °C for 5 h, and (f) $Ni_{20}Co_{27}Sn_{53}$ alloy annealed at 700 °C for 5 h

Table 2 Equilibrium composition of the Ni-Co-Sn ternary system at 700 °C determined in the present work

Alloy/ at%	Annealed time/h	Phase equilibrium	Composition/at%					
		Phase 1/Phase 2/Phase 3	Phase 1		Phase 2		Phase 3	
			Ni	Co	Ni	Co	Ni	Co
$Ni_{11}Co_{70}Sn_{19}$	720	(αCo, Ni)/(Ni, Co)$_3$Sn$_2$	4.75	92.63	19.95	40.03	...	…
$Ni_{10}Co_{56}Sn_{34}$	720	(αCo, Ni)/(Ni, Co)$_3$Sn$_2$	1.44	96.25	12.02	47.33	…	…
$Ni_{16}Co_{42}Sn_{42}$	720	(Ni, Co)$_3$Sn$_2$	16.01	42.24	…	…	…	…
$Ni_{29}Co_{32}Sn_{39}$	720	(Ni, Co)$_3$Sn$_2$	29.35	30.68	…	…	…	…
$Ni_{44}Co_{18}Sn_{38}$	720	(Ni, Co)$_3$Sn$_2$	46.37	14.62	…	…	…	…
$Ni_{65}Co_{12}Sn_{23}$	720	(αCo, Ni)/Ni$_3$Sn(l)	29.88	68.85	68.39	6.61	…	…
$Ni_{10}Co_{30}Sn_{60}$	5	L/CoSn	0.24	1.16	11.77	39.05	…	…
$Ni_{20}Co_{20}Sn_{60}$	5	L/Ni$_3$Sn$_4$	1.17	0.88	24.16	21.35	…	…
$Ni_{30}Co_{10}Sn_{60}$	5	L/Ni$_3$Sn$_4$	1.4	0.76	27.16	18.82	…	…
$Ni_{62}Co_{11}Sn_{27}$	720	(αCo, Ni)/(Ni, Co)$_3$Sn$_2$/Ni$_3$Sn(l)	33.89	65.15	59.68	2.7	68.45	6.39
$Ni_{50}Co_{23}Sn_{27}$	720	(αCo, Ni)/(Ni, Co)$_3$Sn$_2$	32.29	66.55	58.19	3.84	…	…
$Ni_{30}Co_{43}Sn_{27}$	720	(αCo, Ni)/(Ni, Co)$_3$Sn$_2$	7.78	91.16	40.9	20.03	…	…
$Ni_{75}Co_{11}Sn_{14}$	720	(αCo, Ni)/Ni$_3$Sn(l)	73.84	25.37	71.46	3.81	…	…
$Ni_{20}Co_{32}Sn_{48}$	720	(Ni, Co)$_3$Sn$_2$/CoSn	22.19	35.83	14.06	36.57	…	…
$Ni_{27}Co_{25}Sn_{48}$	720	(Ni, Co)$_3$Sn$_2$/Ni$_3$Sn$_4$	29.19	28.19	27.15	20.63	…	…
$Ni_{24}Co_{31}Sn_{45}$	720	(Ni, Co)$_3$Sn$_2$/Ni$_3$Sn$_4$	25.09	33.42	25.29	23.27	…	…
$Ni_{20}Co_{27}Sn_{53}$	5	L/CoSn/Ni$_3$Sn$_4$	0.97	1.07	15.80	34.58	22.81	23.90

annealed at 700 °C for 720 h is shown in Fig.3c. According to the determined phase composition $Ni_{62}Co_{11}Sn_{27}$ alloy showed a three-phases co-existence of [(αCo, Sn) + (Ni, Co)$_3$Sn$_2$ + Ni$_3$Sn(l)]. The corresponding XRD pattern, as shown in Fig. 4b, all the diffraction peaks of the (αCo, Sn), (Ni, Co)$_3$Sn$_2$ and Ni$_3$Sn(l) phases was presented. A two-phase microstructure of [(αCo, Sn)+Ni$_3$Sn(l)] was found in the $Ni_{73}Co_{11}Sn_{14}$ alloy annealed at 700 °C for 720 h, as indicated in Fig. 3d, where the (αCo, Sn) phase with the flat plate shape distributes in the matrix of the Ni$_3$Sn(l) phase. The corresponding XRD pattern, as presented in Fig.4c, showed all the diffraction peaks of the (αCo, Sn) and Ni$_3$Sn(l) phases. The $Ni_{10}Co_{30}Sn_{60}$ alloy annealed at 700 °C for 5 h has formed a two-phase microstructure of CoSn phase and liquid phase, as illustrated in Fig.3e. Fig.3f shows a three-phase microstructure (CoSn+Ni$_3$Sn$_4$+ Liquid phase) of the $Ni_{20}Co_{27}Sn_{53}$ alloy annealed at 700 °C for 5 h.

Based on the above experimental data, the corresponding phase compositions of the annealed alloys is summarized in Table 2, while the 700 °C isothermal section of Ni-Co-Sn ternary system is constructed and shown in Fig.5. In total, two three-phase regions of [(αCo, Sn) + (Ni, Co)$_3$Sn$_2$ + Ni$_3$Sn(l)] and [Ni$_3$Sn$_4$ + CoSn + L], and one liquid region were experimentally confirmed at 700 °C and they were marked with different symbols. An undetermined three-phase regions of [Ni$_3$Sn$_4$ + CoSn + (Ni, Co)$_3$Sn$_2$] was labeled in dashed lines. As can be seen in Fig.5, the solubility of Sn in the (Ni, Co)$_3$Sn$_2$ phase was about 39 at% to 42 at%. The solubility of Co in the Ni$_3$Sn(l) and Ni$_3$Sn$_4$ phase was measured to be about 6.9 at% and 25.6 at%, respectively. The solubility of Ni in the linear compound CoSn phase was about 15.9 at%. The Ni-Co side presents an interconnected (αCo, Sn) phase region.

2.3 Phase equilibria at 1000 °C

Fig.6 presents some typical BSE images of the Ni-Co-Sn alloys annealed at 1000 °C for 168 h or 2 h. As shown in Fig. 6a, two different phases were found in the $Ni_{65}Co_{12}Sn_{23}$ alloy annealed at 1000 °C for 168 h.

Combined with the composition analysis, the light gray phase was identified as Ni$_3$Sn(h), and the black phase was (αCo, Sn) phase. The corresponding XRD pattern, as presented in Fig.7a, shows all the diffraction peaks of the (αCo, Sn) and Ni$_3$Sn(h) phases. Fig.6b shows a BSE image of the $Ni_{62}Co_{11}Sn_{27}$ alloy annealed at 1000 °C for 168 h, where the two-phase equilibrium [Ni$_3$Sn(h) + (Ni, Co)$_3$Sn$_2$] was identified. The corresponding XRD pattern is shown in Fig.7b, the characteristic diffraction peaks of the (Ni, Co)$_3$Sn$_2$ and Ni$_3$Sn(h) phases are only confirmed. In the $Ni_{59}Co_{13}Sn_{28}$ alloy annealed at 1000 °C for 168 h, a three-phase equilibrium [(αCo, Sn)(black) + Ni$_3$Sn(h)(gray) + (Ni, Co)$_3$Sn$_2$(white)] was found as shown in Fig.6c. The corresponding XRD pattern, as presented in Fig.7c, shows all the diffraction peaks of the (αCo, Sn), Ni$_3$Sn(h) and (Ni, Co)$_3$Sn$_2$ phases. Moreover, as it can be seen in Fig.6d, there is a two-phase equilibrium [(Ni,

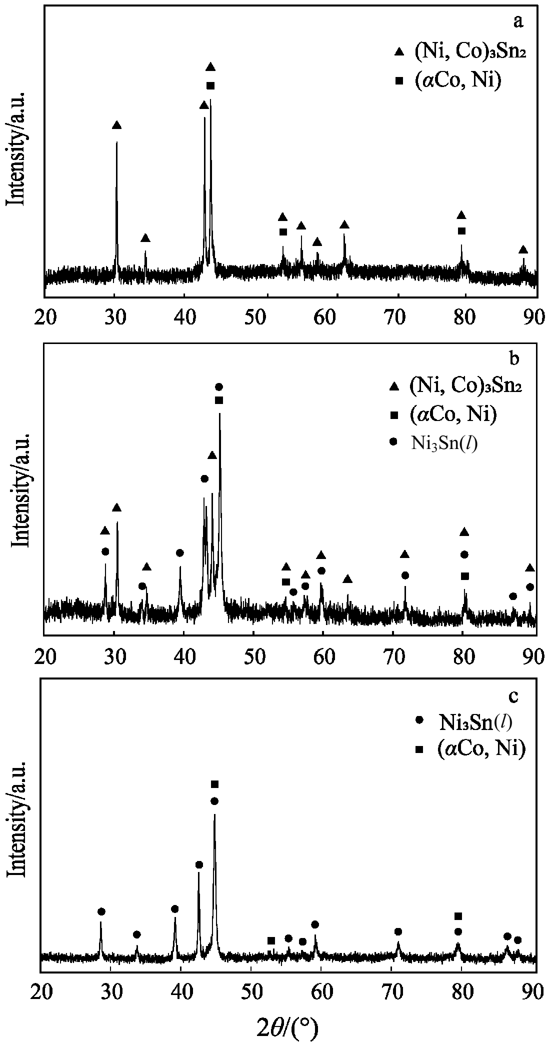

Fig.4 XRD patterns of partial Ni-Co-Sn ternary alloy obtained from $Ni_{11}Co_{70}Sn_{19}$ (a), $Ni_{24}Co_{11}Sn_{27}$ (b), $Ni_{75}Co_{11}Sn_{14}$ alloys (c) annealed at 700 °C

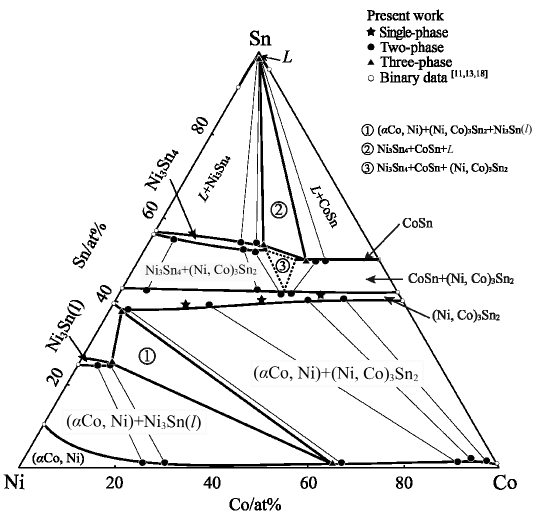

Fig.5 Experimentally determined isothermal section of the Ni-Co-Sn system at 700 °C

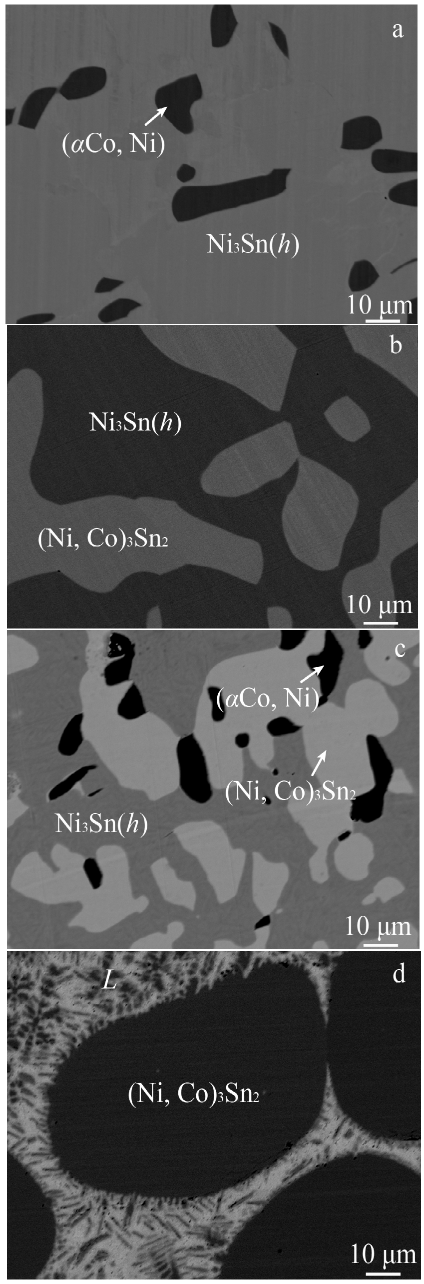

Fig.6 Typical ternary BSE images obtained from Ni-Co-Sn ternary alloys: (a) $Ni_{65}Co_{12}Sn_{23}$ alloy annealed at 1000 °C for 168 h, (b) $Ni_{62}Co_{11}Sn_{27}$ alloy annealed at 1000 °C for 168 h, (c) $Ni_{59}Co_{13}Sn_{28}$ alloy annealed at 1000 °C for 168 h, and (d) $Ni_{10}Co_{30}Sn_{60}$ alloy annealed at 1000 °C for 2 h

$Co)_3Sn_2$ + L] occurring in the $Ni_{10}Co_{30}Sn_{60}$ alloy annealed at 1000 °C for 2 h.

The corresponding phase composition of the annealed alloys is summarized in Table 3, and the 1000 °C isothermal section was established as presented in Fig.8. Only one three-phase regions of [(αCo, Sn) + Ni_3Sn(h) + $(Ni,Co)_3Sn_2$] was found.

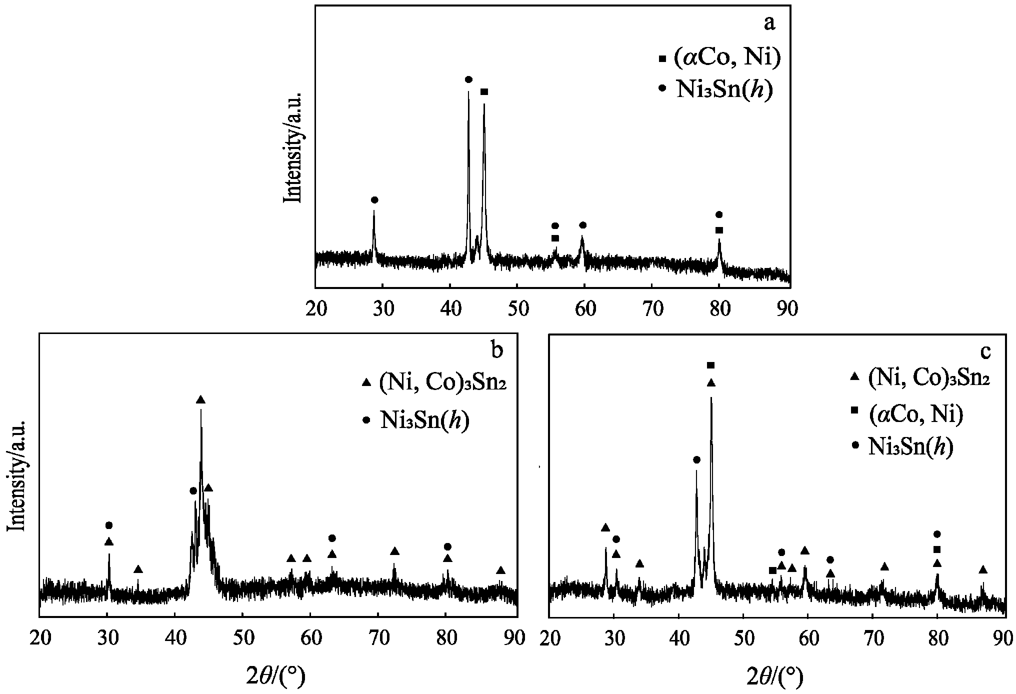

Fig.7 XRD patterns of partial Ni-Co-Sn ternary alloy obtained from $Ni_{65}Co_{12}Sn_{23}$ (a), $Ni_{62}Co_{11}Sn_{27}$ (b), and $Ni_{59}Co_{13}Sn_{28}$ alloys (c) annealed at 1000 °C

Table 3 Equilibrium composition of the Ni-Co-Sn ternary system at 700 °C determined in the present work

Alloy/ at %	Annealing time/h	Phase equilibrium	Composition/at%					
		Phase 1/Phase 2/Phase 3	Phase 1		Phase 2		Phase 3	
			Ni	Co	Ni	Co	Ni	Co
$Ni_{11}Co_{70}Sn_{19}$	168	(αCo, Ni)/(Ni, Co)$_3$Sn$_2$	4.6	93.64	18.15	42.97	…	…
$Ni_{10}Co_{56}Sn_{34}$	168	(αCo, Ni)/(Ni, Co)$_3$Sn$_2$	2.65	95.45	11.24	49.9	…	…
$Ni_{16}Co_{42}Sn_{42}$	168	(Ni, Co)$_3$Sn$_2$	30.95	30.1	…	…	…	…
$Ni_{29}Co_{32}Sn_{39}$	168	(Ni, Co)$_3$Sn$_2$	16.32	42.58	…	…	…	…
$Ni_{44}Co_{18}Sn_{38}$	168	(Ni, Co)$_3$Sn$_2$	45.81	15.97	…	…	…	…
$Ni_{65}Co_{12}Sn_{23}$	168	(αCo, Ni)/Ni$_3$Sn(h)	63.79	30.63	68.2	7.8	…	…
$Ni_{10}Co_{30}Sn_{60}$	2	L/(Ni, Co)$_3$Sn$_2$	12.36	7.77	22.79	35.12	…	…
$Ni_{20}Co_{20}Sn_{60}$	2	L/(Ni, Co)$_3$Sn$_2$	13.88	6.81	26.15	31.82	…	…
$Ni_{62}Co_{11}Sn_{27}$	168	Ni$_3$Sn(h)/(Ni, Co)$_3$Sn$_2$	62.47	12.13	57.47	5.82	…	…
$Ni_{63}Co_{13}Sn_{24}$	168	(αCo, Ni)/Ni$_3$Sn(h)	51.2	45.03	63.44	11.6	…	…
$Ni_{50}Co_{23}Sn_{27}$	168	(αCo, Ni)/(Ni, Co)$_3$Sn$_2$	38.91	56.28	53.42	8.89	…	…
$Ni_{30}Co_{43}Sn_{27}$	168	(αCo, Ni)/(Ni, Co)$_3$Sn$_2$	13.71	83.25	36.99	24.06	…	…
$Ni_{75}Co_{11}Sn_{14}$	168	(αCo, Ni)/Ni$_3$Sn(h)	76.68	15.66	68.26	7.48	…	…
$Ni_{59}Co_{13}Sn_{28}$	168	(αCo, Ni)/ (Ni, Co)$_3$Sn$_2$/Ni$_3$Sn(h)	46.14	50.30	56.72	6.73	60.10	13.64
$Ni_{61}Co_{15}Sn_{24}$	168	(αCo, Ni)/Ni$_3$Sn(h)	48.77	47.53	61.90	13.36	…	…
$Ni_{50}Co_{5}Sn_{45}$	2	L/(Ni, Co)$_3$Sn$_2$	23.26	1.66	51.21	4.98	…	…
$Ni_{40}Co_{15}Sn_{45}$	2	L/(Ni, Co)$_3$Sn$_2$	18.33	3.85	41.24	15.06	…	…

With the temperature increasing from 700 to 1000 °C, there are several differences as summarized in the following: (1) Ni_3Sn_4 phase and CoSn phase disappeared at 1000 °C. (2) According to the Ni-Sn binary phase diagram, the crystal structure of the Ni_3Sn phase changed from Ni_3Sn(l) to Ni_3Sn(h) at 1000 °C. The solubility of Co in the Ni_3Sn(l) phase was measured to be about 6.9 at% at 700 °C and in the Ni_3Sn(h) was measured to be about 15.5 at%. (3) The liquid phase on the Sn-rich side has increased.

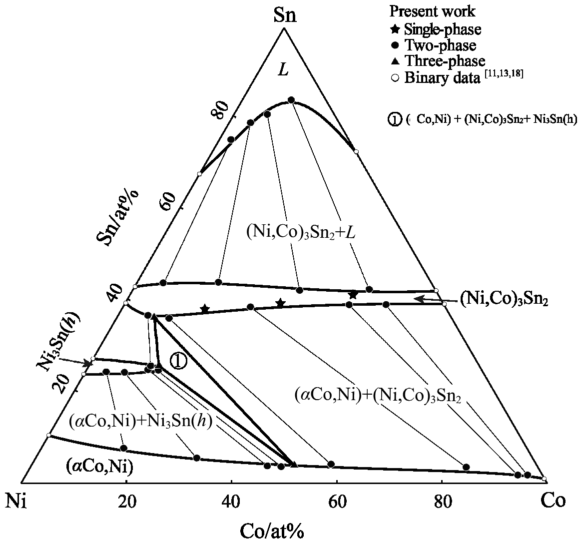

Fig.8 Experimentally determined isothermal section of the Ni-Co-Sn system at 1000 °C

3 Conclusions

1) The isothermal sections of the Ni-Co-Sn ternary system at 700 and 1000 °C have been experimentally investigated. No any ternary compound is found.

2) There is an extensive region of mutual solubility existing between βCo_3Sn_2 phase and $Ni_3Sn_2(h)$ phase, which is labeled as (Ni, Co)$_3$Sn$_2$. The (Ni, Co)$_3$Sn$_2$ phase is a stable phase with dissolving about 39 at% to 42 at% Sn.

3) Three Ni-Sn binary compounds [$Ni_3Sn(l)$, $Ni_3Sn(h)$ and Ni_3Sn_4] show absolutely different solubilities of Co. The $Ni_3Sn(l)$ phase is stable at 700 °C dissolving 6.9 at% Co but it is replaced by the $Ni_3Sn(h)$ phase at 1000°C, and the solubility of Co changed to 15.5 at%. The maximum solubility of Co in Ni_3Sn_4 phase at 700 °C is 25.6 at%, and the Ni_3Sn_4 phase disappears at 1000 °C.

4) The Ni-Co side presents an interconnected (αCo, Ni) phase region at both 700 and 1000 °C and its solubility for Sn is from 1 at% to 10.5 at%. The solubility of Ni in the linear compound CoSn phase is about 15.9 at%.

References

1 Moon K W, Boettinger W J, Kattner U R *et al*. *Journal of Electronic Materials*[J], 2000, 29: 1122
2 Wu C M L, Yu D Q, Law C M T *et al. Materials Science & Engineering R*[J], 2004, 44(1): 1
3 Chao Y H, Chen S W, Chang C H *et al. Metallurgical & Materials Transactions A*[J], 2008, 39: 477
4 Guo K F, Kang H, Ping Q U. *Electronic Components & Materials*[J], 2006, 25: 1
5 Huang Y C, Chen S W. *Journal of Materials Research*[J], 2010, 25: 2430
6 Chen X, Zhou J, Xue F *et al. Journal of Electronic Materials*[J], 2015, 44: 725
7 Yang Y, Balaraju J N, Huang Y *et al. Acta Materialia*[J], 2014, 71: 69
8 Hammad A E. *Microelectronics Reliability*[J], 2018, 87: 133
9 Chen S W, Chang J S, Kevin P *et al. Metallurgical & Materials Transactions A*[J], 2013, 44: 1656
10 Chen Y K, Hsu C M, Chen S W *et al. Metallurgical & Materials Transactions A*[J], 2012, 43: 3586
11 Jen S U, Huang Y R. *Journal of Applied Physics*[J], 1991, 69: 4674
12 Kainuma R, Ise M, Jia C C *et al. Intermetallics*[J], 1996, 4: S151
13 Jiang M, Sato J, Ohnuma I *et al. Calphad-computer Coupling of Phase Diagrams & Thermochemistry*[J], 2004, 28: 213
14 Schmetterer C, Flandorfer H, Richter K W *et al. Journal of Electronic Materials*[J], 2007, 36: 1415
15 Ghosh G. *Metallurgical & Materials Transactions A*[J], 1999, 30: 1481
16 Liu H S, Wang J, Jin Z P. *Calphad-computer Coupling of Phase Diagrams & Thermochemistry*[J], 2004, 28: 363
17 Dong H Q, Vuorinen V, Laurila T *et al. Calphad-computer Coupling of Phase Diagrams & Thermochemistry*[J], 2013, 43: 61
18 Zemanova A, Kroupa A, Dinsdale A. *Monatshefte für Chemie-Chemical Monthly*[J], 2012, 143: 1255

Ni-Co-Sn 三元系相平衡的实验研究

刘兴军[1,2]，邓育灵[1]，张锦彬[1]，杨木金[1]，杨水源[1]，韩佳甲[1]，卢 勇[1]，王翠萍[1]

(1. 厦门大学 材料学院 福建省材料基因工程重点实验室，福建 厦门 361005)

(2. 哈尔滨工业大学 深圳研究院，广东 深圳 518055)

摘 要：采用电子探针显微分析和X-ray衍射分析方法研究了Ni-Co-Sn三元体系在700和1000 ℃时的相平衡。在这两个温度截面中均未发现三元化合物。βCo_3Sn_2相和$Ni_3Sn_2(h)$相形成了一个贯穿连续固溶体相。Ni-Sn侧包含$Ni_3Sn(l)$、$Ni_3Sn(h)$和Ni_3Sn_4 3个化合物相，它们中Sn的固溶度是有很大区别的。700 ℃时，Co在$Ni_3Sn(l)$和Ni_3Sn_4中的最大固溶度分别约为6.9 at%和25.6 at%，在1000 ℃时，Co在$Ni_3Sn(h)$中的最大固溶度约为15.5 at%。在700和1000 ℃下，Ni-Co侧的(αCo, Ni)相为一个贯穿连续固溶体相，并且Sn在(αCo, Ni)相中的固溶度为1 at% ~10.5 at%。Ni在线性化合物CoSn相中的溶解度约为15.9 at%。

关键词：Ni-Co-Sn三元系；相平衡；线性化合物

作者简介：刘兴军，男，1962 年生，博士，教授，厦门大学材料学院，福建 厦门 361005，电话：0592-2187888，E-mail: lxj@xmu.edu.cn